Generalized Dyson model: Nature of the zero mode and its implication in dynamics

Giuseppe De Tomasi, Sthitadhi Roy, and Soumya Bera
Max-Planck-Institut für Physik komplexer Systeme, Nöthnitzer Straße 38, 01187 Dresden, Germany
(Received 10 June 2016; published 6 October 2016)

We study the role of the anomalous $E = 0$ state in dynamical properties of noninteracting fermionic chains with chiral symmetry and correlated bond disorder in one dimension. These models possess a diverging density of states at zero energy leading to a divergent localization length at the band center. By analytically calculating the localization length for a finite system, we show that correlations in the disorder modify the spatial decay of the $E = 0$ state from being quasilocalized to extended. We numerically simulate charge and entanglement propagation and provide evidence that states close to $E = 0$ dominate the dynamical properties. Remarkably, we find that correlations lead to subdiffusive charge propagation, whereas the growth of entanglement is logarithmically slow. A logarithmic scaling of entanglement saturation with system size is also observed, which indicates a behavior akin to quantum critical glasses.

DOI: 10.1103/PhysRevB.94.144202

I. INTRODUCTION

In one-dimensional disordered systems, the presence of a chiral symmetry (sublattice) can lead to some energy eigenstates behaving differently than all other localized eigenstates. For instance, a bond disordered model, which we refer to as the Dyson I model [1,2], has a diverging density of states at $E = 0$, which is accompanied with a divergent localization length [3–5]. Although the localization length is diverging, the state is quasilocalized because the localization length scales subextensively with system size [6,7]. Another mechanism in disordered systems that can modify the nature of its eigenstates is the presence of correlations in disorder. Even with on-site disorder, where all single-particle eigenstates are exponentially localized in one dimension [8,9], correlations in the disorder can either partially or completely destroy localization [10–17]. Moreover, the study of correlated disorder has several practical applications, particularly in transport properties of disordered conducting polymers and biological molecules [18,19].

The combination of symmetries and disorder correlations can have interesting effects in the physics of Anderson localization. For instance, bond dimerization (referred to as Dyson II model [20] hereafter), i.e., random bonds appearing in identical pairs ($J_{2l-1}=J_{2l}$; J_l is the bond strength), changes the nature of the $E = 0$ state from being quasilocalized to extended. Despite this, the role of local disorder correlations with regard to the nature of the $E = 0$ state and the consequent effect on nonequilibrium dynamical properties has not been explored extensively so far. In this article, we construct and study a random bond model with tunable correlated bond disorder, such that the spatial extension of the $E = 0$ state can be modified almost continuously from being exponentially localized to extended. The construction also allows us to recover the known Dyson I and II models in appropriate limits. We further examine the effect of the nature of the $E = 0$ state on the transport properties via charge and entanglement propagation.

Recently, dynamical properties of isolated disordered systems have attracted much attention due to advancement of controlled experimental techniques as well as the discovery of dynamical quantum phase transitions. In particular, dynamical properties are used to characterize different localized phases. For example, in both the Anderson localized and the many-body localized (MBL) phase [21,22] charge transport is absent. However, while in the former the bipartite entanglement $\mathcal{S}(t)$ does not grow with time, in the latter it grows logarithmically [23,24]. Furthermore, it has been shown that, while in the ergodic phase of the MBL system charge and entanglement show subdiffusive and subballistic behavior, respectively [25,26], in a diffusive nonintegrable spin chain $\mathcal{S}(t)$ grows ballistically with time [27]. It is then natural to conclude that charge and entanglement propagation can have different dynamical behaviors, which further motivates us to contrast them in the presence of both disorder correlation and symmetries. Interestingly, the generalized Dyson model shows subdiffusive density propagation and logarithmic entanglement growth, a phenomenon that has not been observed previously in disordered systems.

The rest of the paper is organized as follows. In the Sec. II, we introduce the generalized model and analytically derive the localization length of the $E = 0$ state, and describe the phase diagram with regard to the localization properties. We describe the dynamical properties in Sec. III, with Sec. III A containing the numerical results for the Dyson II limit while the results for other parameter values are presented in Sec. III B. Finally, the results are summarized in Sec. IV.

II. MODEL AND LOCALIZATION LENGTH

The nearest-neighbor random hopping model is defined as

$$\mathcal{H} = -\sum_{l}[J_{2l-1}c^{\dagger}_{2l-1}c_{2l} + J_{2l}c^{\dagger}_{2l}c_{2l+1} + \text{H.c.}], \qquad (1)$$

where $c^{\dagger}_l$ (c_l) is the fermionic creation (annihilation) operator at site l and J_ls are positive random hopping amplitudes. The Hamiltonian (1) with uncorrelated disorder has a diverging mean density of states $\varrho(E) \sim 1/E\log^3(E)$ as $E \to 0$ [1,28,29], which also leads to a logarithmic divergence in the localization length with energy [4,20]. Several independent correlation lengths also diverge for the $E = 0$ state [30,31], indicating that the state serves as a disorder-induced quantum critical point. In dynamical properties, the quasilocal nature of the state manifests itself in extremely slow propagation of charge [32] and entanglement growth $\sim \log[\log(t)]$ [33–35].

We start by investigating the localization length of the model (1) using the transfer matrix technique. To this end, we define $\xi_L(E)$ as the localization length of a finite system of size L at energy E. We choose L odd with open boundary condition as it guarantees the existence of an $E=0$ state due to sublattice symmetry [36]. Generically, $\xi_L(E=0)$ can be expressed using the recursion relations between single-particle wave function amplitudes as

$$\xi_L^{-1}(E=0)=\frac{1}{L}\overline{\log\left|\frac{\psi_{L-1}}{\psi_0}\right|}=\frac{1}{L}\sum_{l=1}^{\frac{L-1}{2}}\overline{\log\left(\frac{J_{2l}}{J_{2l-1}}\right)}, \quad (2)$$

where the overline denotes the disorder average. For uncorrelated disorder, e.g., the Dyson I model, the average of the summation in Eq. (2) is zero. However, in a typical configuration the sum is divergent with system size L, which indicates that one needs to investigate the full probability distribution of the sequence under the sum rather than just the mean. Using the central limit theorem, it can be shown that the fluctuations grow as $\sqrt{L}$ and therefore $\xi_L(E=0)\sim\sqrt{L}$ [16,17]. On the contrary, in the presence of dimerization, $J_{2l-1}=J_{2l}$, the Dyson II model, the sum in Eq. (2) is zero for *each* configuration. Consequently $\psi_{L-1}=\psi_0$ implying that the $E=0$ state is extended in all samples [20]. With the motivation of interpolating between these two limits of quasilocalized (Dyson I) and extended (Dyson II) $E=0$ states, we choose the random couplings as

$$J_{2l-1}=\mathcal{B}^{(1)}_{2l-1}\exp\left[\frac{-\eta_{2l-1}\mathcal{B}^{(2)}_{2l-1}}{(2l-1)^\alpha}\right],$$
$$J_{2l}=\mathcal{B}^{(1)}_{2l-1}\exp\left[\frac{\eta_{2l}\mathcal{B}^{(2)}_{2l}}{(2l)^\alpha}\right], \quad (3)$$

where $\mathcal{B}^{(1)}_l$, $\mathcal{B}^{(2)}_l$ are random variables drawn from Gamma distributions with unit mean and variance $1/W_{(1,2)}$ defined as

$$P_W(x)=\frac{W^W}{\Gamma(W)}x^{W-1}e^{-Wx},\ x\geqslant 0, \quad (4)$$

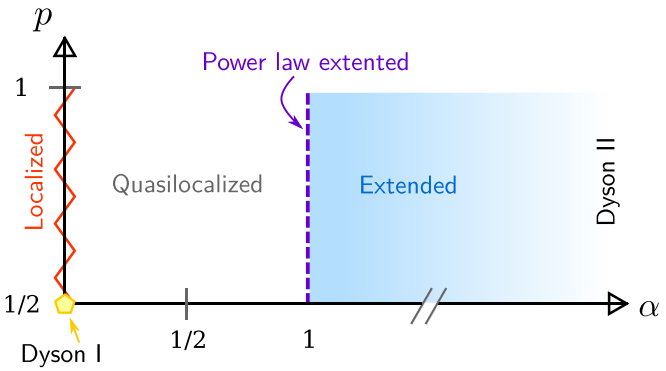

FIG. 1. Phase diagram with regard to the asymptotic behavior of the $E=0$ state. The regimes denoted by "Localized" ("Extended") have localized (extended) $E=0$ state. For $\alpha=0$, $p=1/2$ limit we recover the (uncorrelated) Dyson model and also for $\alpha>1$, the dimerized Dyson II model is restored. See text for further details of the localization length in Eq. (6) and Eq. (8).

where $\Gamma(W)$ is the Gamma function. η_l's are independent random variables with the probability density function $\rho(\eta)=p\delta(\eta-1)+(1-p)\delta(\eta+1)$ with $p\in[\frac{1}{2},1]$, and $\alpha\geqslant 0$. J_l's are short-range-correlated random variables and inhomogeneous in space. The inhomogeneity is predominantly in the edge of the sample, while in the bulk it is suppressed. With this choice of J_l's, Eq. (2) reduces to

$$\log\left|\frac{\psi_{L-1}}{\psi_0}\right|=\sum_{l=1}^{L-1}\frac{\eta_l\mathcal{B}^{(2)}_l}{l^\alpha}. \quad (5)$$

In Eq. (5), α and p determine the asymptotic behavior of $\xi_L(E=0)$ as the thermodynamic limit is approached and also allows us to change the extension of the $E=0$ state almost continuously.

For $p\neq 1/2$ and $\alpha\geqslant 0$, averaging over the disorder and approximating the sum in Eq. (5) as an integral in the large-L limit, we get

$$\xi_L(E=0)\sim\begin{cases}(2p-1)^{-1}L^\alpha, & 0\leqslant\alpha<1,\\ (2p-1)^{-1}L/\log L, & \alpha=1,\\ (2p-1)^{-1}L, & \alpha>1,\end{cases} \quad (6)$$

which immediately identifies four distinct regimes. For $\alpha=0$, $\xi_L(E=0)$ is finite, which leads to an exponentially localized state. In the range $0<\alpha<1$, the localization length diverges algebraically but slower than the system size, which we refer to as a quasilocalized state (see also Fig. 1). The logarithmic correction to $\xi_L(E=0)$ at $\alpha=1$ produces a polynomial spatial decay of the wave function. In the limit $\alpha\to\infty$, the correlation reveals itself via the dimerization of bonds, $J_{2l-1}=J_{2l}$, which is the Dyson II model with an extended $E=0$ state.

For $p=1/2$, the sign η_l appears with equal probability. Therefore, $\xi_L^{-1}(E=0)$ defined in Eq. (2) goes to zero upon taking disorder average. Hence, in order to understand the asymptotic behavior of $\xi_L^{-1}(E=0)$, we analyze the fluctuations of the sequence $\{\log|\psi_{L-1}/\psi_0|\}$, similar to the Dyson I model as follows. Let $\mathcal{A}_L$ be the random variable defined after averaging over $\mathcal{B}^{(2)}_l$'s in Eq. (5),

$$\mathcal{A}_L=\overline{\left[\log\left|\frac{\psi_{L-1}}{\psi_0}\right|\right]}=\sum_{l=1}^{L-1}\frac{\eta_l}{l^\alpha}. \quad (7)$$

$\mathcal{A}_L$ is a sum of independent but not identically distributed random variables with zero mean and variance $\sigma_l^2=1/l^{2\alpha}$. The *Lyapunov central limit theorem* [37] then dictates that the probability distribution of $\mathcal{A}_L$ approaches to a Gaussian distribution with zero mean and variance, $\sigma^2_{\mathcal{A}_L}=\sum_{l=1}^{L-1}l^{-2\alpha}$, in the limit $L\to\infty$. The asymptotic behavior of $\sigma^2_{\mathcal{A}_L}$ can then be used to extract the behavior of the localization length,

$$\xi_L(E=0)\propto L\sigma_{\mathcal{A}_L}\sim\begin{cases}L^{\alpha+1/2}, & 0\leqslant\alpha<1/2,\\ L/\sqrt{\log L}, & \alpha=1/2,\\ L, & \alpha>1/2.\end{cases} \quad (8)$$

Three qualitatively different regimes can be identified. For $0\leqslant\alpha<1/2$, the localization length diverges algebraically, but slower than the system size. At the $\alpha=0$, $p=1/2$ point, we recover the Dyson I model, where the localization length diverges as $\sim\sqrt{L}$ solely due to fluctuations. Finally, for $\alpha>1/2$, the state is extended with system size. The behavior

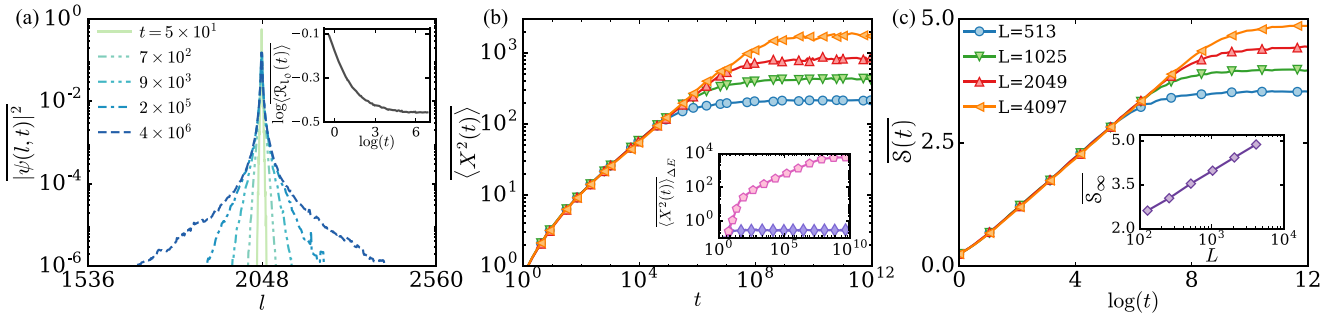

FIG. 2. (a) The disorder-averaged wave packet at different times for the Dyson II model. The central core decays quickly and saturates after initial dynamics, whereas the tail of the distribution keeps spreading with time. Inset shows the return probability for $L = 4097$. (b) The growth of $\overline{\langle X^2(t)\rangle}$ with time for $L = \{513, \ldots, 4097\}$ in log-log scale. For finite systems it saturates to a value which grows linearly with the system size. Inset shows $\overline{\langle X^2(t)\rangle}_{\Delta E}$ with $E = 0$ present ($\pentagon$) in ΔE which grows subdiffusively and absent ($\diamondsuit$) which saturates, hence confirming that the dynamics is governed by the states close to $E = 0$ ($L = 4097$). (c) The entanglement entropy shows a logarithmic growth in time $\overline{\mathcal{S}(t)} \sim \log t$ and the saturation, $\overline{\mathcal{S}_\infty}$, grows logarithmically with L as shown in the inset.

of $\xi_L(E = 0)$ as a function of α and p is summarized in Fig. 1. Importantly, the phase diagram is stable against any local perturbations that do not break the original symmetry of the $\mathcal{H}$, because it does not qualitatively change the structure of Eq. (2).

III. DYNAMICAL PROPERTIES

Having established that the model (1) with the random couplings (3) hosts several different natures of extended/quasilocalized state at $E = 0$, we now investigate its effects on dynamical properties. First, we study charge propagation via wave packet dynamics in the single-particle framework [38–41]. The initial wave packet is localized at a single point l_0 in the middle of the chain, $\psi(l,t = 0) = \delta_{l,l_0}$. With time it spreads out and its amplitude at the initial site l_0 decays. We monitor the decay of the initial density via the return probability $\langle \mathcal{R}_{l_0}(t)\rangle = |\psi(l_0,t)|^2$ and quantify the spreading of the charge by the disordered average mean-square displacement $\overline{\langle X^2(t)\rangle} = \sum_l l^2 \overline{|\psi(l,t)|^2} - [\sum_l l \overline{|\psi(l,t)|^2}]^2$. Furthermore, the growth of bipartite entanglement entropy $\mathcal{S}(t) = -\mathrm{Tr}\{\rho_{\mathrm{L}}(t)\log[\rho_{\mathrm{L}}(t)]\}$ between two halves of the system L and R is investigated using standard free fermion techniques [42], where $\rho_{\mathrm{L}}(t) = \mathrm{Tr}_{\mathrm{R}}[|\psi(t)\rangle\langle\psi(t)|]$ and $|\psi(t=0)\rangle$ is a random product state at half filling. Under time evolution, L and R subsystems exchange information leading to the growth of $\mathcal{S}(t)$, which is zero at $t = 0$. In our simulations, we use open boundary conditions with $W_1 = 0.4$ and $W_2 = 10$, and checked (not shown) that with periodic boundary condition, even number of sites, and also with other values of $W_{(1,2)}$ there are no qualitative difference in the conclusions.

A. Dyson II ($\alpha \to \infty$)

Since the dynamical properties of these localized systems are expected to be dominated by the properties of the states close to $E = 0$, it is expected that the dynamics would be qualitatively different depending on which regime of the phase diagram they belong to. We first focus on the Dyson II model with dimerized hopping. In Fig. 2(a) we show the probability distribution of the time-dependent wave function at different times. At long times only the tail of the wave function keeps spreading, while the return probability saturates after an algebraic decay as seen in the inset. Finite $\overline{\langle \mathcal{R}_{l_0}(t)\rangle}$ at long times implies a finite density of exponentially localized states in the energy spectrum [43].

Figure 2(b) shows the expansion of the width of the wave packet. The linear behavior of the width with time in log-log scale suggests $\overline{\langle X^2(t)\rangle} \sim t^\beta$, where the nonuniversal exponent β depends on the disorder strength, e.g., $\beta \approx 0.35$ for $W_1 = 0.4$, which implies subdiffusion. For finite systems, the growth saturates, with the saturation value growing linearly with the system size reflecting the spatial extension of the $E = 0$ state (6).

Note that due to the diverging nature of the density of states, the dynamics is always going to be dominated by a finite number of states in the vicinity of $E = 0$. We ascertain this by projecting the initial wave packet onto eigenstates within an energy window ΔE that includes $E = 0$ and also away from it as $|\psi_0\rangle_{\Delta E} = \hat{P}_{\Delta E}|\psi(l_0,t=0)\rangle$, where $\hat{P}_{\Delta E} = \sum_{E\in\Delta E}|E\rangle\langle E|$ and $|E\rangle$ is the eigenstate. We contrast the two situations by measuring the spread of the wave packet as $\overline{\langle X^2(t)\rangle}_{\Delta E} = \overline{\langle\psi_0|_{\Delta E}\hat{X}^2(t)|\psi_0\rangle_{\Delta E}} - \overline{\langle\psi_0|_{\Delta E}\hat{X}^2(0)|\psi_0\rangle_{\Delta E}}$. As seen in the inset of Fig. 2(b) the spectral decomposed wave packet with the $E = 0$ state shows a subdiffusive propagation ($\pentagon$), whereas the wave packet that has been projected away from the band center quickly saturates ($\diamondsuit$) as one would expect for localized states.

Figure 2(c) shows the growth of disorder-averaged bipartite entanglement $\overline{\mathcal{S}(t)}$ starting from a product state. We observe a logarithmic growth of $\overline{\mathcal{S}(t)}$ in time, which is slower than the charge transport. For $W_1 = 0.4$ the prefactor of $\log(t)$ is $\approx \ln(2)/3$. In the inset of Fig. 2(c) the saturation value of $\overline{\mathcal{S}(t)}$ at $t \to \infty$ ($\overline{\mathcal{S}_\infty}$) is plotted in a log-linear scale, which shows logarithmic scaling with system size with a slope $\approx \ln(2)$. The logarithmic scaling of $\overline{\mathcal{S}_\infty}$ is similar to entanglement scaling of critical states. Unlike in an interacting localized phase, where entanglement is generated via dephasing due to interaction [23,24], here it is due to the extended nature of the $E = 0$ state, which implies that the saturation time of

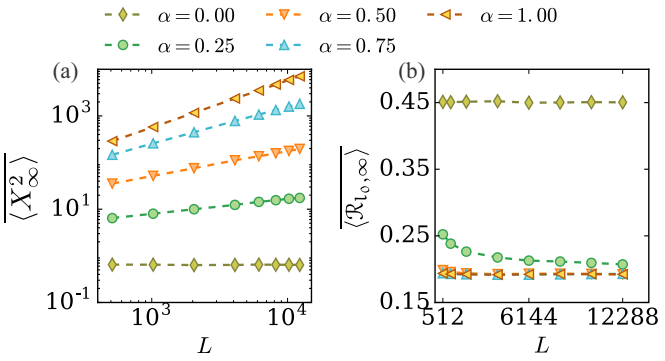

FIG. 3. (a) $\overline{\langle X^2_\infty \rangle}$ for different values of α in a log-log scale to highlight the scaling $\propto L^\alpha$ as expected from the localization length calculation (6). (b) The return probability $\overline{\langle \mathcal{R}_{l_0,\infty} \rangle}$ (9) for different α shows saturation with system size L. Dashed lines are given as guides to the eye.

$\mathcal{S}(t)$ is proportional to the localization length of the extended state.

Note that there is no qualitative change in our results at higher values of W_1. Specifically for $W_1 > 1$, when the Gamma distribution (4) becomes nonsingular at zero, $\overline{\langle X^2(t) \rangle}$ and $\overline{\mathcal{S}(t)}$ still show a subdiffusive and logarithmic growth in time, respectively, as shown in the Appendix.

B. $0 \leqslant \alpha \leqslant 1$, $p = 1$

For any finite α, charge propagation is subdiffusive. The difference for different α is seen in the scaling of the saturation values of $\overline{\langle \mathcal{R}_{l_0,\infty} \rangle}$ and $\overline{\langle X^2_\infty \rangle}$ with L, as the localization lengths depend on α. Figure 3(a) shows the $t \to \infty$ value of the width of the wave packet in a log-log plot as a function of system size. The leading behavior is given by L^α as one would expect from the extended nature of the $E = 0$ eigenstate described in Eq. (6). Crudely approximating the $E = 0$ eigenstate, $|\phi_0\rangle$, as a box function of width $\xi_L(E = 0)$, one finds $\langle \phi_0 | \hat{X}^2 | \phi_0 \rangle \propto \xi_L(E = 0)$. Similarly, in Fig. 3(b) we show the return probability at $t \to \infty$, defined as

$$\langle \mathcal{R}_{l_0}(t) \rangle = |\psi(l_0,t)|^2 \xrightarrow{t=\infty} \sum_n |\phi_n(l_0)|^4, \tag{9}$$

which is the inverse participation ratio of the single-particle eigenstates. Two things are of note: (i) for $0 \leqslant \alpha \leqslant 1$, it converges with L, which emphasizes that most of the eigenstates are localized, (ii) for $\alpha = 0$, the $\overline{\langle \mathcal{R}_{l_0,\infty} \rangle}$ converges at a different value than other α's. This can be understood from the following decomposition of inverse participation ratio (9), $\sum_n |\phi_n(l_0)|^4 = \sum_{n<|\Delta E|} |\phi_n(l_0)|^4 + \sum_{n>|\Delta E|} |\phi_n(l_0)|^4$, where ΔE is the window of energies enclosing delocalized states around $E = 0$. Only for $\alpha \neq 0$ the first term in the sum is negligible because of the extended nature of the states within the interval ΔE; however for $\alpha = 0$, $\Delta E = 0$ as all states are localized (6). Therefore, it is expected that $\alpha = 0$ converges at a higher value as seen in Fig. 3(b) compared to other α.

Figure 4(a) shows the time evolution of $\overline{\mathcal{S}(t)}$ for different values of α after a global quench. The data show a logarithmic growth of entanglement similar to Dyson II. Note that the slope at which $\mathcal{S}(t)$ grows is almost independent of α, while

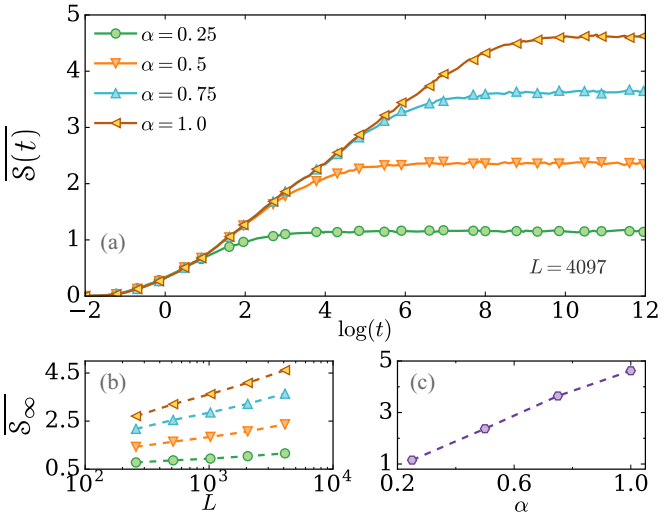

FIG. 4. (a) Dynamics of entanglement for different values of α and $p = 1$ in a log-linear scale after a quench from a product state. The logarithmic growth of $\overline{\mathcal{S}(t)}$ is visible for all values of α shown here. (b) The saturation value of $\overline{\mathcal{S}(t)}$ at long time behaves as $\log(L)$ for all $\alpha \neq 0$. (c) The entanglement saturation $\overline{\mathcal{S}_\infty}$ shows a linear growth with α ($L = 4097$) (10).

the effect of α is clearly visible in the saturation. To highlight the dependence of the saturation with system size we plot $\overline{\mathcal{S}_\infty}$ as a function of L in Fig. 4(b) in log-linear scale. For $\alpha > 0$ we see a logarithmic increase of $\overline{\mathcal{S}_\infty}$ with a slope $\propto \alpha$. This is further confirmed in Fig. 4(c), where the saturation of entanglement is plotted as a function of α. The behavior

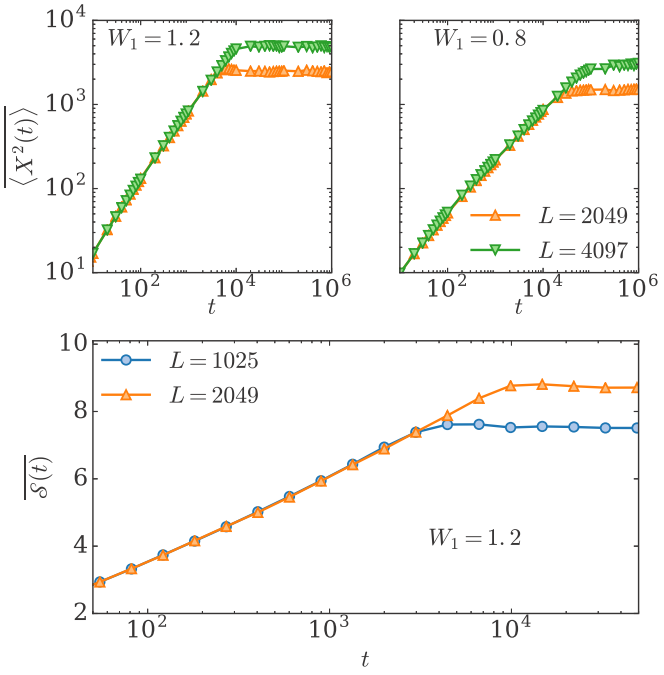

FIG. 5. Top: The subdiffusive growth of $\overline{\langle X^2(t) \rangle}$ for the Dyson II model in log-log scale for two different values of W_1 and for two different system sizes $L = 2049,4097$. Bottom: Logarithmic growth of $\overline{\mathcal{S}(t)}$ for the Dyson II model for $W_1 = 1.2$ and $L = 1025,2049$.

suggests the following form of $\mathcal{S}(t)$ with time and system size,

$$\overline{\mathcal{S}(t)} \sim \log(t), \quad \overline{\mathcal{S}_\infty} \sim \log[\xi_{L,\alpha}(E=0)], \tag{10}$$

where $\xi_{L,\alpha}(E=0)$ is the localization length and is $\propto L^\alpha$ (6). For $\alpha = 0$, $p > 1/2$ the state is exponentially localized and therefore neither charge or entanglement propagate.

IV. CONCLUSION

In summary, we have constructed a generalized correlated one-dimensional random bond disorder model and studied its nonequilibrium dynamics. Even though the localization length of the $E = 0$ state is divergent, the state can be quasilocalized or extended and its spatial extent depends on the correlations in disorder. We have shown that the dynamical properties are dominated by the states close to $E = 0$. In all the parameter regimes studied we find subdiffusive transport, while logarithmically slow growth of entanglement. The saturation value of the wave packet and entanglement depends on the finite-size localization length of the $E = 0$ state. In particular, $\overline{\mathcal{S}_\infty}$ grows logarithmically with the localization length of the $E = 0$ state. The scaling behavior is similar to the scaling of $\mathcal{S}$ in the excited state of uncorrelated random spin chain in the same universality class [44,45], except that in our generalized model disorder correlation enters in the $\overline{\mathcal{S}_\infty}$ scaling via the finite-size localization length of the $E = 0$ state.

ACKNOWLEDGMENTS

We thank A. Bäcker, D. Bagrets, A. Croy, F. Evers, A. Lazarides, R. Singh, and J-M. Stéphan for several illuminating discussions. We also express our gratitude to J. H. Bardarson, F. Evers, and F. Pollmann for a critical reading of the manuscript.

APPENDIX: RESULTS FOR DIFFERENT DISORDER STRENGTHS

In this appendix we show additional results for different values of W_1 for the Dyson II model. They further substantiate our conclusions about subdiffusive wave packet dynamics, and logarithmically slow entanglement growth in the generalized model. Figure 5 (top) shows the growth of $\overline{\langle X^2(t)\rangle}$ for the Dyson II model for $W_1 = 0.8$ and $W_1 = 1.2$. For both these values of W_1, $\overline{\langle X^2(t)\rangle}$ grows algebraically with time, $\overline{\langle X^2(t)\rangle} \sim t^{\beta(W_1)}$, with $\beta(W_1 = 1.2) \approx 0.78$ and $\beta(W_1 = 0.8) \approx 0.59$, showing the subdiffusive dynamics. Figure 5 (bottom) shows that the growth of $\overline{\mathcal{S}(t)}$ for the Dyson II model with $W_1 = 1.2$. It is still clearly visible that the entanglement growth in time is logarithmic, $\overline{\mathcal{S}(t)} \sim \log(t)$. Note that, for $W_1 = 1.2$, the Gamma distribution is no longer singular at zero, yet we see subdiffusive wave packet dynamics and logarithmic entanglement growth, ensuring that this behavior is indeed generic.

[1] F. J. Dyson, Phys. Rev. **92**, 1331 (1953).
[2] M. Weissmann and N. V. Cohan, J. Phys. C **8**, L145 (1975).
[3] R. L. Bush, J. Phys. C **8**, L547 (1975).
[4] G. Theodorou and M. H. Cohen, Phys. Rev. B **13**, 4597 (1976).
[5] T. P. Eggarter and R. Riedinger, Phys. Rev. B **18**, 569 (1978).
[6] L. Fleishman and D. C. Licciardello, J. Phys. C **10**, L125 (1977).
[7] C. M. Soukoulis and E. N. Economou, Phys. Rev. B **24**, 5698 (1981).
[8] N. Mott and W. Twose, Adv. Phys. **10**, 107 (1961).
[9] I. Y. Gol'dshtein, S. A. Molchanov, and L. A. Pastur, Functional Analysis and Its Applications **11**, 1 (1977).
[10] D. H. Dunlap, H.-L. Wu, and P. W. Phillips, Phys. Rev. Lett. **65**, 88 (1990).
[11] F. A. B. F. de Moura and M. L. Lyra, Phys. Rev. Lett. **81**, 3735 (1998).
[12] F. M. Izrailev and A. A. Krokhin, Phys. Rev. Lett. **82**, 4062 (1999).
[13] H. Shima, T. Nomura, and T. Nakayama, Phys. Rev. B **70**, 075116 (2004).
[14] U. Kuhl, F. M. Izrailev, and A. A. Krokhin, Phys. Rev. Lett. **100**, 126402 (2008).
[15] A. Croy, P. Cain, and M. Schreiber, Eur. Phys. J. B **82**, 107 (2011).
[16] F. Izrailev, A. Krokhin, and N. Makarov, Phys. Rep. **512**, 125 (2012).
[17] H. Cheraghchi, S. M. Fazeli, and K. Esfarjani, Phys. Rev. B **72**, 174207 (2005).
[18] D. Klotsa, R. A. Römer, and M. S. Turner, Biophys. J. **89**, 2187 (2005).
[19] A. A. Krokhin, V. M. K. Bagci, F. M. Izrailev, O. V. Usatenko, and V. A. Yampol'skii, Phys. Rev. B **80**, 085420 (2009).
[20] T. A. L. Ziman, Phys. Rev. Lett. **49**, 337 (1982).
[21] D. M. Basko, I. L. Aleiner, and B. L. Altshuler, Ann. Phys. **321**, 1126 (2006).
[22] I. V. Gornyi, A. D. Mirlin, and D. G. Polyakov, Phys. Rev. Lett. **95**, 206603 (2005).
[23] J. H. Bardarson, F. Pollmann, and J. E. Moore, Phys. Rev. Lett. **109**, 017202 (2012).
[24] M. Serbyn, Z. Papić, and D. A. Abanin, Phys. Rev. Lett. **110**, 260601 (2013).
[25] Y. Bar Lev, G. Cohen, and D. R. Reichman, Phys. Rev. Lett. **114**, 100601 (2015).
[26] D. J. Luitz, N. Laflorencie, and F. Alet, Phys. Rev. B **93**, 060201 (2016).
[27] H. Kim and D. A. Huse, Phys. Rev. Lett. **111**, 127205 (2013).
[28] A. Ovchinnikov and N. Erikhman, JETP **46**, 340 (1977).
[29] P. W. Brouwer, C. Mudry, and A. Furusaki, Phys. Rev. Lett. **84**, 2913 (2000).
[30] D. S. Fisher, Phys. Rev. B **50**, 3799 (1994).
[31] D. S. Fisher, Phys. Rev. B **51**, 6411 (1995).
[32] P. L. Krapivsky and J. M. Luck, J. Stat. Mech.: Theory Exp. (2011), P02031.
[33] G. D. Chiara, S. Montangero, P. Calabrese, and R. Fazio, J. Stat. Mech.: Theory Exp. (2006), P03001.

[34] R. Vosk and E. Altman, Phys. Rev. Lett. **110**, 067204 (2013).
[35] Y. Zhao, F. Andraschko, and J. Sirker, Phys. Rev. B **93**, 205146 (2016).
[36] With our system sizes we do not observe any even-odd effects in the dynamics. This is because the single-particle energy level spacing close to $E = 0$ becomes exponentially small with L .
[37] L. Koralov and Y. G. Sinai, *Theory of Probability and Random Processes* (Springer Science and Business Media, 2007).
[38] F. M. Izrailev, T. Kottos, A. Politi, and G. P. Tsironis, Phys. Rev. E **55**, 4951 (1997).
[39] R. Ketzmerick, K. Kruse, S. Kraut, and T. Geisel, Phys. Rev. Lett. **79**, 1959 (1997).
[40] B. Huckestein and R. Klesse, Phys. Rev. B **59**, 9714 (1999).
[41] R. P. A. Lima, F. A. B. F. de Moura, M. L. Lyra, and H. N. Nazareno, Phys. Rev. B **71**, 235112 (2005).
[42] I. Peschel, J. Phys. A **36**, L205 (2003).
[43] Using numerical transfer matrix calculation, we checked that at other energies ($E \neq 0$) corresponding Lyapunov exponents are strictly positive.
[44] Y. Huang and J. E. Moore, Phys. Rev. B **90**, 220202 (2014).
[45] R. Vasseur, A. C. Potter, and S. A. Parameswaran, Phys. Rev. Lett. **114**, 217201 (2015).